A&A manuscript no.
(will be inserted by hand later)

Your thesaurus codes are:
06(08.09.2; 08.15.1; 08.22.3; 03.13.2; 03.13.4; 02.03.1;)

ASTRONOMY
AND
ASTROPHYSICS
1.2.2008

Analysis of the Irregular Pulsations of AC Her

Z. Kolláth @2 @1 ⋆, J. R. Buchler @1 ⋆⋆, T. Serre @3 & J. Mattei @4

@1 Physics Department, University of Florida, Gainesville, FL 32611 @2 Konkoly Observatory, Budapest, Hungary
@3 Observatoire de Paris, Meudon, France @4 AAVSO, Cambridge, MA 02138

June 1997

Abstract. The AAVSO lightcurve data of the irregularly pulsating star AC Herculis of the RV Tau class are analysed. The lightcurve is shown to be incompatible with a periodic, or even multiperiodic pulsation, even if allowance is made for evolution. Instead the best explanation is that the irregularly alternating cycles are a manifestation of low dimensional chaos. The lightcurve is found to be generated by a 3 or 4 dimensional dynamics – 3 or 4 first order ODEs. The (Lyapunov) fractal dimension of the underlying dynamic attractor is computed to be $d_L \approx 2.2$, smaller than the value of $d_L \approx 3.1$ found for R Sct.

Key words: Stars: individual: AC Her – Stars: oscillations – Stars: variable: others – Methods: data analysis – Methods: numerical – Chaos

1. INTRODUCTION

In this paper we analyze the AAVSO data set of the lightcurve of AC Herculis that shows irregular pulsations with large cycle to cycle alternations in the lightcurve. The paper is organized in parallel to the analysis of R Scuti (Buchler, Serre, Kolláth & Mattei 1995 hereafter BSKM, Buchler, Kolláth, Serre & Mattei 1996, hereafter BKSM). Despite their membership in the same RV Tau class the lightcurves of these two stars are quite different. AC Her has a period of 35 days, about half that of R Sct, has a much lower pulsation amplitude, and is much less irregular. From a practical point of view, the available AAVSO data set is shorter, there are more gaps and fewer points per cycle, and the relative noise level is higher, all of which make the analysis harder.

In §2 we show that the pulsations are incompatible with periodic or multiperiodic behavior, even when evolution is allowed for. The pulsations must therefore be either of a chaotic or of a stochastic nature. (We follow the general trend of distinguishing the two by calling chaotic an erratic signal that is generated by a deterministic low dimensional dynamics whose form can be found, at least in principle, and stochastic a very high dimensional dynamics that is too complicated to be characterized otherwise than stochastically.) In §3 we perform a nonlinear analysis that shows that the observational data are indeed compatible with low dimensional chaos, and we determine its quantitative properties. This is followed by a discussion in §4, and we conclude in §5.

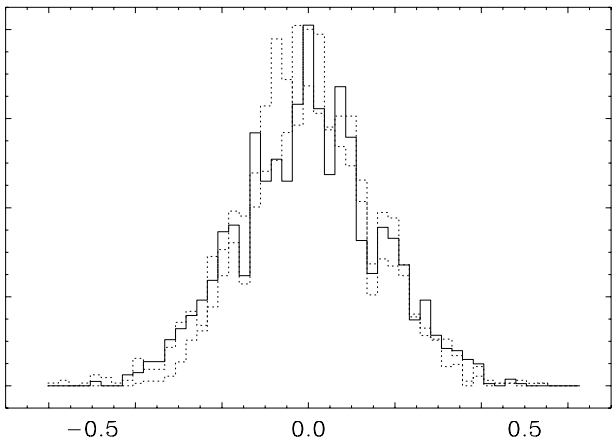

Fig. 1. Error distributions of the AAVSO data; data grouped into 3 ranges, below, in and above 7.5 to 7.8 mag.

2. Standard Analysis

For a description of the AAVSO observational data archive we refer to Percy and Mattei 1993. The data set of visual observations spans JD2437596 – 2449442. For most of our nonlinear analyses we use only the second part (after JD2445000) of the data where the data coverage is better. The average (rms) error of the data is quite large, about 0.15 mag. However, the errors are found to have a Gaussian distribution, independent of *magnitude*, but not

⋆ e–mail address: kollath@buda.konkoly.hu
⋆⋆ e–mail address: buchler@phys.ufl.edu

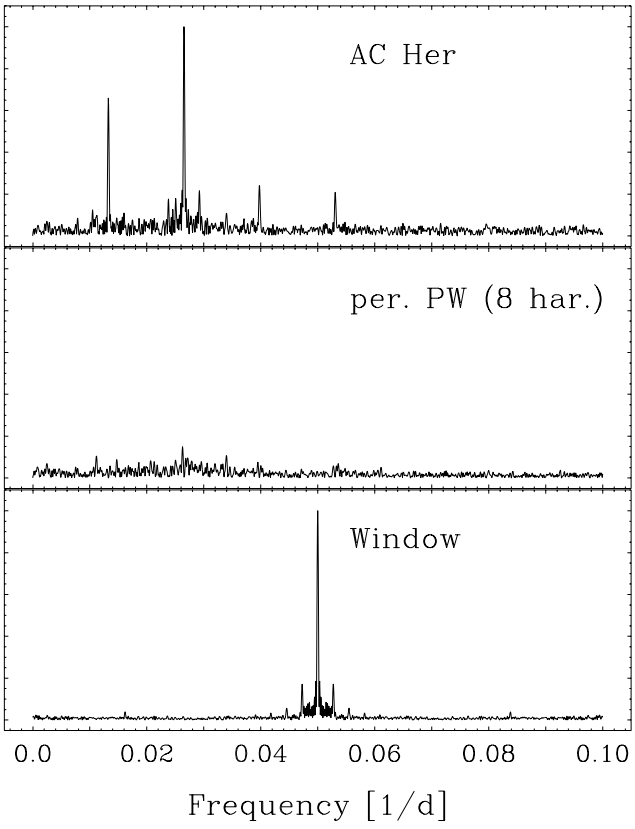

Fig. 2a. Fourier Spectra. *Top row:* AAVSO data; *2nd row:* periodic prewhitening with f_0 and 7 harmonics (same ordinate scale); *3rd row:* spectral window.

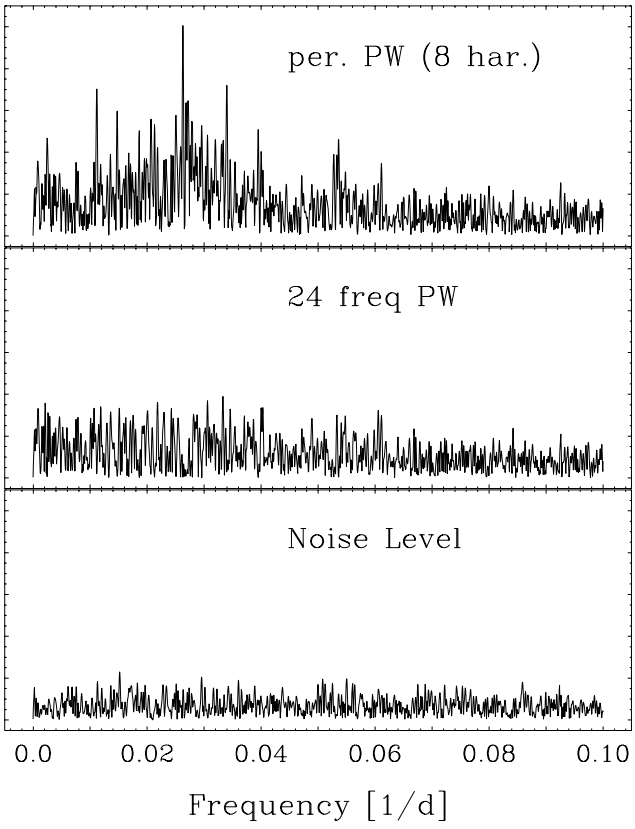

Fig. 2b. Fourier Spectra; *Top row:* periodic prewhitening with f_0 and 7 harmonics; *2nd row:* multiperiodic prewhitening with f_0 and 7 harmonics plus the 23 most important independent frequencies; *bottom row:* expected observational noise level; all three figures have the same ordinate scale.

of luminosity, which is a reflection of the visual nature of the observations. This is quite apparent from Fig. 1 where we have superposed the histograms for the errors for the data spit into three groups, viz. below, in and above the range 7.5 – 7.8 mag. Just as for R Sct we therefore analyze the magnitude rather than the more physical luminosity. It is thanks to the Gaussian error distribution that in the next section we are able to extract a relatively good average signal from the bare data.

In Fig. 2a, on top, we display the *amplitude* Fourier spectrum (FS) of the averaged AAVSO data for the observed AC Her lightcurve. The spectrum is clearly dominated by four peaks. The fundamental frequency peak is located at f_0=0.01326 d^{-1} (P_0=75.43 d).

In the bottom row we show the spectral window which introduces some of the side-lobe structure that is evident in the top figure.

Prima facie the FS of AC Her seems to suggest periodicity (as does the lack of phase jumps in the pulsations, cf. Fig. 5 below). Therefore, in the second row we show the FS of the lightcurve with a periodic prewhitening with f_0 and 7 harmonics. (Actually the last, highest four harmonics improve the prewhitening very little). The phases of the three dominant harmonics, Φ_k, k=1, 3 vary in concordance with Φ_0 over the time span of the data (see Fig. 3 where we show Φ_0 and Φ_1). This establishes a strong harmonic or perhaps resonant connection among the four dominant peaks. However, the 'grass' in the FS is very high, and furthermore the lightcurve has several observationally well established local features that a periodic fit completely misses.

To investigate the possibly noisy origin of the left-over grass we take the periodic component (that has been used in the prewhitening of the second row of Fig. 2b) and add simulated Gaussian observational noise, with an intensity as indicated by the AAVSO data, viz. $\approx$ 0.15 mag. The FS of a prewhitened realization of such a noisy periodic signal is shown in the bottom row of Fig. 2b. Note that the ordinate scales of figures 2a and 2b are different. For comparison the same, periodically prewhitened FS is therefore shown in both figures.

Could the pulsations be multiperiodic instead of periodic? To answer this question we first allow the eight dominant frequencies (i.e. f_0 and previously its harmonics) to be independent. This multiperiodic prewhitening produces essentially no reduction in the grass of the FS compared to the periodic prewhitening, nor does it improve the fit to the data. Next we make a more extensive prewhitening using now f_0 and its 7 harmonics plus 24 *linearly independent* frequencies, chosen from the highest peaks in row 2 of Fig. 2a. The resultant FS is shown in the second row FS of Fig. 2b. Despite this large number of frequencies quite a bit of unresolved grass still remains in the FS that cannot be explained away as observational noise as a comparison with the last row indicates. In addition, an overlay of the 24–periodic fit on the AAVSO data shows that many significant features are still missed.

Furthermore one would be hard-pressed theoretically to explain the origin of 24 or more frequencies of oscillation in this star, particularly if the star is undergoing radial pulsations, as expected. Even if nonradial pulsations are involved and these visual observations could resolve up to ℓ=2 modes, it would not be possible to account for all these 'observed' frequencies.

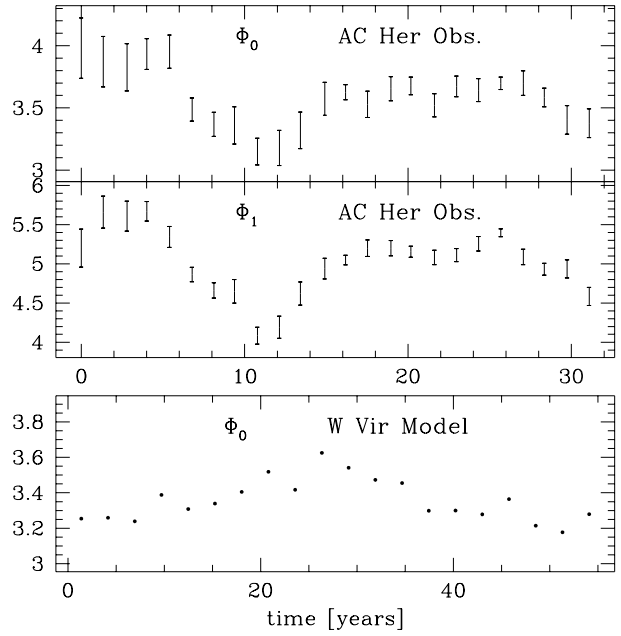

Fig. 3. *Top:* Time-dependence of the phases Φ_0 and Φ_1 over the span of the AC Her data set, *bottom:* Variation of the phase Φ_0 with time over the span of a corresponding data set of W Vir numerical model pulsations.

The lightcurve therefore *cannot reasonably be explained as being periodic or multiperiodic with constant frequencies*.

Could the star be undergoing noticeable evolution over the decade that the data span? Fig. 3 reports the time-dependence of the phases Φ_0 and Φ_1 of the lightcurve for the frequencies f_0 and $f_1 = 2f_0$. Here we have used the whole AAVSO dataset. Were one to interpret the phase variations as due to evolutionary changes in the frequency one might conclude from the two approximately parabolic arcs that the frequency changes linearly in time ($\dot{P}_0 = 4{\times}10^{-4}$), but that in addition there is a very strong frequency glitch around t=11 y. However, one would be hard pressed to come up with a mechanism for such a large glitch. Zsoldos (1988) found a periodic variation in the $O-C$ curve of the minima with a period of 9323 days. We cannot check the existence of this modulation because of the shorter time span of the data. Very recently Percy et al. (1977) have studied the period changes of RV Tauri stars, including AC Her. They concluded that the $O-C$ diagrams can be interpreted as a superposition of random

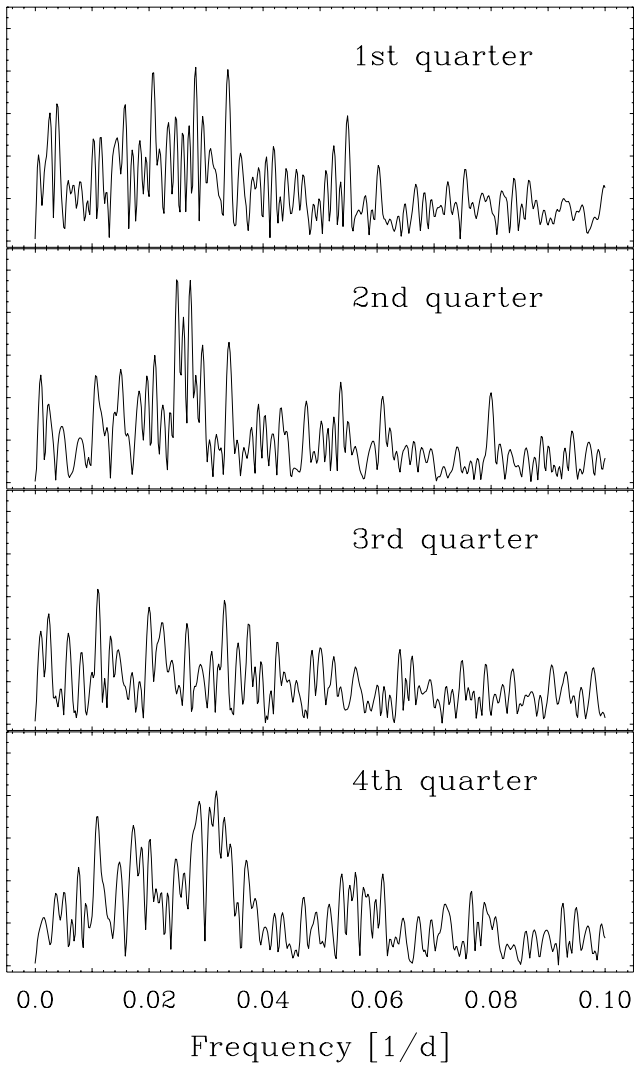

Fig. 4. Fourier Spectra of the prewhitened successive quarter partitions of the AAVSO data.

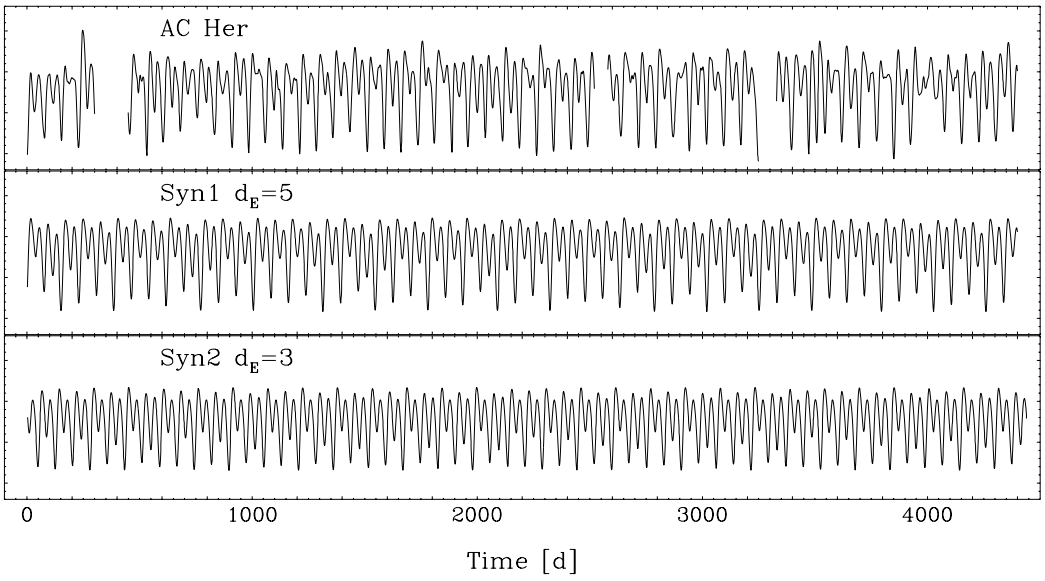

Fig. 5. Lightcurves; *Top*: AC Her, smoothed data (JD 2,445,000 + 4400 d); *Middle:* section of synthetic data from reconstructed global map (d_E=5, Δ=6, p=4, σ=0.065); *Bottom:* synthetic data (d_E=3, Δ=5, p=6, σ=0.065)

errors in the measured times of minimum, and random cycle-to-cycle fluctuations in the period.

If, despite the preceding discussion, one still insisted on interpreting the pulsations as multiperiodic, then one should observe a systematic change in all the frequencies and in the associated amplitudes. We have therefore partitioned the whole AAVSO data set into quarters. Except for f_0 and its three harmonics already considered there is no apparent systematic variation in the grass. Fig. 4 displays the FS of the successive partitions of the data, all prewhitened and scaled the same way as the whole data set that has been shown in the second row of Fig. 2b.

In order to offer an alternative explanation for the phase variations of AC Her, we also show in Fig. 3 the phase variations obtained from the magnitude variations of hydrodynamic simulations of a W Vir model (Kovács & Buchler 1986, Buchler 1993, Gouesbet et al. 1997). Following the same reasoning as for AC Her one might interpret the phase variations again as indicating a linear time dependence of the frequency (increasing with time here), also with an abrupt frequency shift at 27 y. However, here we are absolutely sure that such an interpretation would be incorrect! There is no evolution built into the W Vir model, and the pulsations were definitely shown to be chaotic. The *phase variations are a natural result of the chaotic nature of the pulsations*, and over short time-intervals they can give an erroneous impression of periodicity. We therefore suggest that the apparent piecewise parabolic behavior in AC Her is spurious and that the phase variations have the same chaotic origin.

We thus conclude that the pulsations of *AC Her cannot be explained as those of an evolving multiperiodic star either.*

The presence of spots seems an unlikely explanation for the irregular pulsations of this type of luminous star. There is however the possibility of stochasticity, for example caused by internal convection. It is hard to rule out a nonlinear stochastic process. However, in the spirit of Occam's razor, if a simpler valid explanation can be found we see no need to search for a stochastic description which in any case would just push our ignorance further down the line.

We are thus led to investigate if the pulsations can be due to an underlying low dimensional chaotic dynamics. In a priori support of such an explanation we recall that the recent nonlinear analysis of the R Sct lightcurve as well as the modelling of W Vir models have indicated such chaotic behavior. We therefore now turn to the type of nonlinear analysis that can uncover low dimensional chaos when it is in the data. (We refer a reader who is unfamiliar with chaos to the excellent introduction by Ott 1993, or to general reviews by Weigend & Gershenfeld 1994, Abarbanel et al. 1993).

3. Global Flow Reconstruction

In a recent publication Serre, Kolláth & Buchler (1995, hereafter SKB; see also Buchler 1997 for a lecture note, or Gouesbet et al. 1997 for more general reviews) introduced a nonlinear time-series analysis, the global flow reconstruction method, that is suitable for astronomical

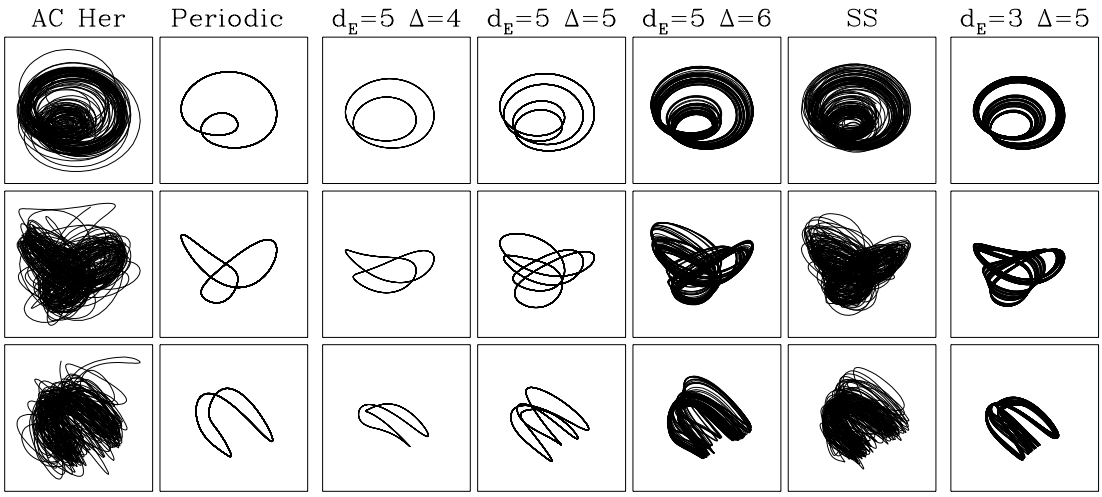

Fig. 6. Broomhead-King projections, from top down: (ξ_2 vs ξ_1), (ξ_3 vs ξ_1), (ξ_3 vs ξ_2); *Col. 1:* smoothed AC Her lightcurve; *Col. 2:* Periodic fit (8 harmonics) to the data; *Cols. 3–5:* Synthetic signals for delay vectors,d_E=5, Δ=4 through 6; *Col. 6:* Synthethic signal of col. 5 (Δ=6) with added noise, sampled, averaged and smoothed like the AC Her data (see text); *Col. 7:* Synthetic signal for d_E=3, Δ=5

data. A prior reading of these papers is suggested, not only for a description of the method but also for the notation and terminology that is used here. The application to the analysis of the lightcurve of R Sct appears in BSKM and BKSM.

For the nonlinear analysis the AAVSO magnitude data first need to be converted into a sequence with equal time-spacings, $\{s(t_n)\}$. We do this by performing 3 day averages that are then cubic-spline smoothed and interpolated with a σ=0.065. For comparison we will also show results with a 5 day average, and with smoothing parameters of σ=0.06 and σ=0.07. The reason for smoothing with a σ that is less than the observational noise is that we have already averaged the data which has introduced some smoothing. The observational data have many gaps, many of which are too large to bridge. We have therefore limited ourselves to the time-interval JD2445000 + 4400 days which has only three gaps (cf. Fig. 5).

Almost all nonlinear analyses start with the construction of 'delay vectors' $\mathbf{X}(t_n) \equiv \mathbf{X}^n = \{s(t_n), s(t_n - \Delta), s(t_n - 2\Delta), \ldots, s(t_n - (d_E - 1)\Delta)\}$, where Δ is the 'delay' and d_E is the dimension of the 'reconstruction space'. The $\mathbf{X}^n$ provide a strobed representation of the 'trajectory' of the system in this d_E–dim space.

We now make the a priori assumption that the light curve is generated by a deterministic nonlinear mechanism of low dimension. Phrased differently, we assume that there is a dynamics that connects neighboring points of the trajectory. A theorem guarantees that there is a one-to-one correspondence between the trajectory in the real or physical phase space of the system and the trajectory in the reconstruction space. Importantly, some of the properties are preserved in this correspondence. It is therefore possible to extract information about the physical dynamics from the observational data of a single observed variable (the luminosity here). All we have to do is to determine the functional form of the flow $d\mathbf{Z}/dt = \mathbf{G}(\mathbf{Z})$ that gives rise to this trajectory $Z(t)$, where the observations provide the strobed values $\mathbf{Z}(t_n) = \mathbf{X}^n$.

A priori we do not know what values to give to Δ and d_E. The delay should be large enough so that the attractor is not squashed into the diagonal, but sufficiently small so that a polynomial nonlinearity can describe the flow. There is a minimum value for d_E, called the embedding dimension, in which the trajectory is resolved, i.e. it is devoid of intersections and cusps. Nothing can be gained in increasing d_E beyond this value, but as a check, the properties of the reconstructed map should stay invariant in higher dimensions. We are of course interested in finding this minimum value because it provides an upper bound on the dimensional of the physical dynamics that underlies the observed signal (SKB).

For the quantitative reconstruction of the flow we turn to the global reconstruction method (SKB). We can equivalently reconstruct either a flow $\mathbf{G}$ or a 'map' $\mathbf{F}$ that connects the neighboring points on the trajectory. In SKB and BKSM we found that generally it is somewhat easier to construct maps, and that is what we do here. Our goal is thus to search for the best global polynomial map $\mathbf{F}$, such that $\mathbf{X}^{n+1} = \mathbf{F}(\mathbf{X}^n)$.

Once we have constructed a map $\mathbf{F}$ we can iterate it and produce 'synthetic' signals that can then be compared

Table 1. Lyapunov exponents and dimension

d_e	Δ	p	σ	λ_1	λ_3	λ_4	λ_5	d_L	
3	5	6	0.065	0.0033	–0.034			2.10	†
3	10	6	0.065	0.0045	–0.026			2.17	
3	13	6	0.065	0.0069	–0.030			2.23	
4	5	5	0.065	0.0073	–0.016	–0.054		2.46	
5	6	4	0.065	0.0045	–0.023	–0.025	–0.032	2.19	†
5	7	4	0.065	0.0075	–0.009	–0.025	–0.056	2.85	
3	13	6	0.060	0.0015	–0.029			2.05	
3	3	6	0.070	0.0021	–0.037			2.06	
3	6	6	0.070	0.0032	–0.024			2.13	
5	6	4	0.070	0.0043	–0.015	–0.025	–0.036	2.29	
3	5	6	0.065	0.0025	–0.017			2.14	*
3	10	6	0.065	0.0013	–0.021			2.06	*
3	13	6	0.065	0.0015	–0.013			2.21	*

Lyapunov exponents in d^{-1}
† shown in Fig. 5
* with 5 day instead of 'standard' 3 day averages of AAVSO data

to the observed lightcurve data. Since both are chaotic signals it would be meaningless to compare them point by point. Instead they need to be compared for their overall properties (cf. SKB, BKSM).

In Fig. 5, rows 2 and 3, we show two of the best synthetic signals that we have been able to construct in 5D and in 3D, respectively. The first has the parameters Δ= 6, p= 4, σ=0.065, d_E= 5, the second, Δ= 5, p= 6, σ=0.065, d_E= 3. (An earlier synthetic signal was already shown in a review by Buchler, Kolláth & Serre, 1995 where we also show the first return maps). The synthetic signals reproduce the data reasonably well, although they are somewhat 'tamer'.

Broomhead-King projections which are projections on the eigenvectors of the correlation matrix (q.v. SKB) provide a means to visualize the signals that is optimal in many ways. Thus in Fig. 6 we display the lowest Broomhead-King (BK) projections for the smoothed AC Her data in Col. 1. From the top down we show successively the projections ξ_2 vs. ξ_1, ξ_3 vs. ξ_1, ξ_3 vs. ξ_2. Col. 2 shows the 8 harmmonic periodic signal that has been used to prewhiten the data earlier on (Fig. 2). This periodic signal clearly represents an average of the data. The BK projections of the good synthetic signals in 5D and 3D that have been shown in Fig. 5 are displayed in Cols. 5 and 7, respectively. The signal of Col. 6 will be discussed below.

We need to pause to say a word about what we mean by 'successful' or 'best' reconstructions. The synthetic signals that we reconstruct with a map generally are limit cycles, sometimes with period doubling (Col. 3), quadrupling (Col. 4), or chaos. We hardly ever encounter fixed point attractors or multi-periodic ones (these could have 2 or 3 frequencies – 2 or at most 3–tori (since we keep $d_E \leq 6$), except when the data are oversmoothed (cf. e.g. BKSM). Thus, the delay Δ=3 gives a limit cycle, whereas with Δ=4 we get a 2-cycle (Col. 3 in Fig. 6), with Δ=5 a 4-cycle (Col. 4) and with Δ=6 a chaotic attractor (Col. 5). We note that the period two or four cycles that precede chaos when a parameter is varied, such as Δ in the preceding example, generally indicate that the parameters of the map are close to what it takes to give chaos, and instead of being detrimental they are an indirect confirmation of chaos.

We have summarized some of the tests in Table 1. The columns denote successively the reconstruction dimension d_E , the delay Δ, the highest order p of the monomials used in the map, and the smoothing parameter in the cubic spline fit to the AAVSO data. Next are shown the Lyapunov exponents of the synthetic signals λ_k, ordered with decreasing magnitudes. Finally, we show the fractal Lyapunov dimension d_L which is an overall measure of the chaos.

We draw attention to the following features: As expected all the $\lambda_1 > 0$, which constitutes a clear indication of chaos. Next, all $\lambda_2 \approx 0$ which because of the high sampling rate corroborates that a flow (autonomous system) underlies the pulsations (cf. SKB). The synthetic signals have reasonably robust properties as we go to higher dimensions $d_E = 4$ and 5 (although for a reason not understood it is a little harder to get good maps in d_E=4 than in 3 or 5). The properties are also reasonably independent of the 'massaging', i.e. averaging, smoothing and interpolating of the observational data.

From the Table it thus transpires that we are able to construct a good map in a reconstruction space as low as d_E=3. However, the map is not quite as good as we can achieve with d_E=4 or 5. It therefore cannot be ruled out that we avoid all intersections and cusps in 3D (cf. SKB).

It is very comforting that the successful reconstructions are stable in the sense that they give comparable properties in higher d_E as Table 1 shows.

We do not display the FS of the synthetic signals, but note that whenever the Lyapunov dimension is in the range 2.1 – 2.2 the spectra compare rather well with the observed spectrum, Fig. 2. The less successful reconstructions, which also yield a higher d_L are shown in the Table, give a FS in which the first peak is very broadened.

Many spurious detections of chaos have been made in the literature, especially when techniques such as correlation dimensions are used, and one should therefore always be wary of such pitfalls. SKB and BKSM did some tests that concluded that it is difficult to fool the global flow reconstruction method into erroneously predicting low-dimensional chaos on a stochastic signal. (More specifically they had applied the method to an average periodic component of the R Sct lightcurve and contaminated with colored noise of same FS as R Sct).

As a test for the stability of the reconstruction for AC Her we perform the following two experiments:

The first one is to take a section of our best chaotic synthetic signal (shown in Fig. 5 (second row) and Fig. 6 (Col. 5) of the same length and sampled as the AAVSO data set, add Gaussian noise with the observational intensity of 0.15 mag, perform a 3 day averaging and a cubic spline smoothing with σ=0.065. The BK projections of this signal are shown in col. 6 of Fig. 6. When this signal is then subjected to the global flow reconstruction: Interestingly, the reconstructed synthetic signal is again chaotic. Its Lyapunov dimension is found to be $d_L \approx 2.2$–2.4, i.e. very close to the values for AC Her lightcurve. It is nevertheless remarkable that this second processing of the signal still yields chaos with similar properties as the first one.

The second test signal is taken to be stochastic. Starting with the periodic, 8 harmonic signal used to prewhiten the AC Her data in Fig. 2a, we added noise with the observational intensity of 0.15 mag. It is gratifying that just as in BKSM, *no* erroneous chaotic synthetic signals are produced by the reconstruction for any of the values of d_E, Δ, p, σ that we have tried.

4. Discussion

In §2 we showed that the lightcurve of AC Her is not compatible with an interpretation of a steady periodic or multiperiodic star, nor with a multiperiodic and evolving one. The next simplest working hypothesis is that the lightcurve is chaotic, i.e. that it is generated by a low dimensional dynamics with chaotic trajectories. In §3 we show that indeed we can explicitly construct dimensional flows with simple polynomial nonlinearities with properties close to the observed AC Her lightcurve. Furthermore, whenever the synthetic solutions resemble the observational data, they have similar Lyapunov exponents and Lyapunov dimension, this independently of reconstruction dimension d_E.

The reconstruction of maps is less robust than it is for R Sct (BKSM). We see several reasons for this.
(a) First, the signal to noise ratio is lower, and the observational error is a little larger, viz. 0.15 as compared to 0.10 for R Sct, because AC Her is fainter. The reconstruction method therefore has greater difficulty reconstructing the attractor from the noise.
(b) The AC Her pulsations are more regular, and the trajectory explores a smaller region of phase space. Especially there is a complete absence of trajectories about the unstable fixed point of the map (or flow). This also has the drawback of determining less well the linear part of the map and the properties of the fixed point; In BKSM we linearized the map to show that its unstable fixed point has 2 spiral roots, one unstable and one stable with the trajectory running away from the fixed point with the fundamental frequency to return toward the fixed point with approximately twice the frequency. This was interpreted as showing that the chaotic behavior of R Sct is the result of the nonlinear interaction of two vibrational modes that are in an approximate resonance. A similar argument is thus not possible here.
(c) The more irregular features in the observational data are too few to have a sufficient influence on the map construction, e.g. the peak near 220 d and the 'unusual' oscillation near 3500 d. These features are also prominent as the few very large excursions in the BK plots of the first column of Fig. 6.

When these wildest excursions are disregarded the AC Her projections and the Δ=6 reconstructions become quite similar. This is quite apparent in the noisy smoother synthetic signal of Col. 6 of Fig. 6 that has already been discussed.

From the inequality $d_L < d \leq d_E$ and the value $d_L \approx 2.2$ that we have determined we conclude (cf. SKB) that the physical Euclidean dimension of the underlying attractor is therefore 4, and perhaps as low as 3.

5. Conclusions

AC Her is the second irregular variable star that we have analyzed with the global flow reconstruction method. Our conclusion is that the pulsations of AC Her are very likely to be the result of low dimensional chaos. However, because of the inferior quality of the observational data the case is not quite as strong as for R Sct for which we have little doubt as to the chaotic nature of the pulsations. We also recall that the numerical hydrodynamical modelling of the pulsations of W Vir type stars (KB88 and Serre, Kolláth & Buchler 1995b) showed very clearly low dimensional chaos.

The applications of nonlinear analyses such as this one are still in their infancies. Furthermore, the available observational data are far from optimal for such applications. Further progress will have to await more specific observing efforts tailored to the type of data that are required by nonlinear analyses, such as long uninterrupted observational spans. We stress however that long seasonal gaps do not pose a problem for nonlinear analyses.

When the results of our analysis of AC Her are compared with those of R Sct, on the one hand, and with the pulsations of W Vir models one notices a trend, which is already obvious from a visual inspection of he lightcurves: As the period increases the alternations in the shallow and deep minima as well as the modulations become increasingly irregular. This behavior is also observed in a quantitative fashion in the Lyapunov dimension that increases from $\approx$ 2.05 for the W Vir model, to $\approx$ 2.2 for AC Her and to $\approx$ 3.1 for R Sct. It appears that one may be able to extract useful quantitative information from an irregular lightcurves. In turn, that this will put novel and very useful constraints on the numerical modelling of

these objects. On the theoretical side a thorough numerical hydrodynamical survey of W Vir and RV Tau models is clearly also necessary to confirm this hope.

6. Acknowledgments

This research has been supported in part by NSF (AST92-18068, AST95-28338, INT94-15868), a Hungarian OTKA grant (F4352), an RDA grant at UF, the French Ministère pour la Recherche et l'Espace, and RCI grant from IBM through UF.

References

Abarbanel, H. D. I., Brown, R., Sidorowich, J. J., Tsimring, L. S. 1993, Rev. Mod. Phys. 65, 1331

Buchler, J. R., 1997, *Search for Low-Dimensional Chaos in Observational Data*, International School of Physics "Enrico Fermi", Course CXXXIII on "*Past and Present Variability of the Solar-Terrestrial System: Measurement, Data Analysis and Theoretical Models*", Eds. G. Cini Castagnoli & A. Provenzale (in press).

Buchler, J.R. 1993, in *Nonlinear Phenomena in Stellar Variability*, p. 9, Eds. M. Takeuti & J.R. Buchler, Dordrecht: Kluwer Publishers, reprinted from 1993, Ap&SS, 210

Buchler, J. R., Serre, T., Kolláth, Z. & Mattei, J. 1995, Phys. Rev. Lett. 74, 842 [BSKM]

Buchler J. R., Kolláth, Z., Serre, T. & Mattei, J. 1996, ApJ 462, 489 [BKSM]

Gouesbet, G., LeSceller, L, Letellier, C., Brown, R., Buchler, J.R. & Kolláth, Z. 1997, *Nonlinear Signal and Image Processing*, Ann. N.Y. Acad. Sci. Vol. 808, p. 25.

Kovács, G. & Buchler, J. R. 1988, ApJ, 334, 971, [KB88].

Ott, E. 1993, *Chaos in Dynamical Systems* (Univ. Press: Cambridge)

Percy, J.R., Bezuhly, M. Milanowski, M. & Zsoldos, E. 1997. PASP 109, 264

Percy, J.R. & Mattei, J.A. 1993. Ap&SS 210, 137 PASP 109, 264

Serre, T., Kolláth, Z. & Buchler, J. R. 1995a, A&A 311, 833 [SKB]

Serre, T., Kolláth, Z. & Buchler, J. R. 1995b, A&A 311, 845

Weigend, A. S. & Gershenfeld, N. A. 1994, *Time Series Prediction* (Reading: Addison-Wesley)

Zsoldos, E. 1988, IBVS, 3192

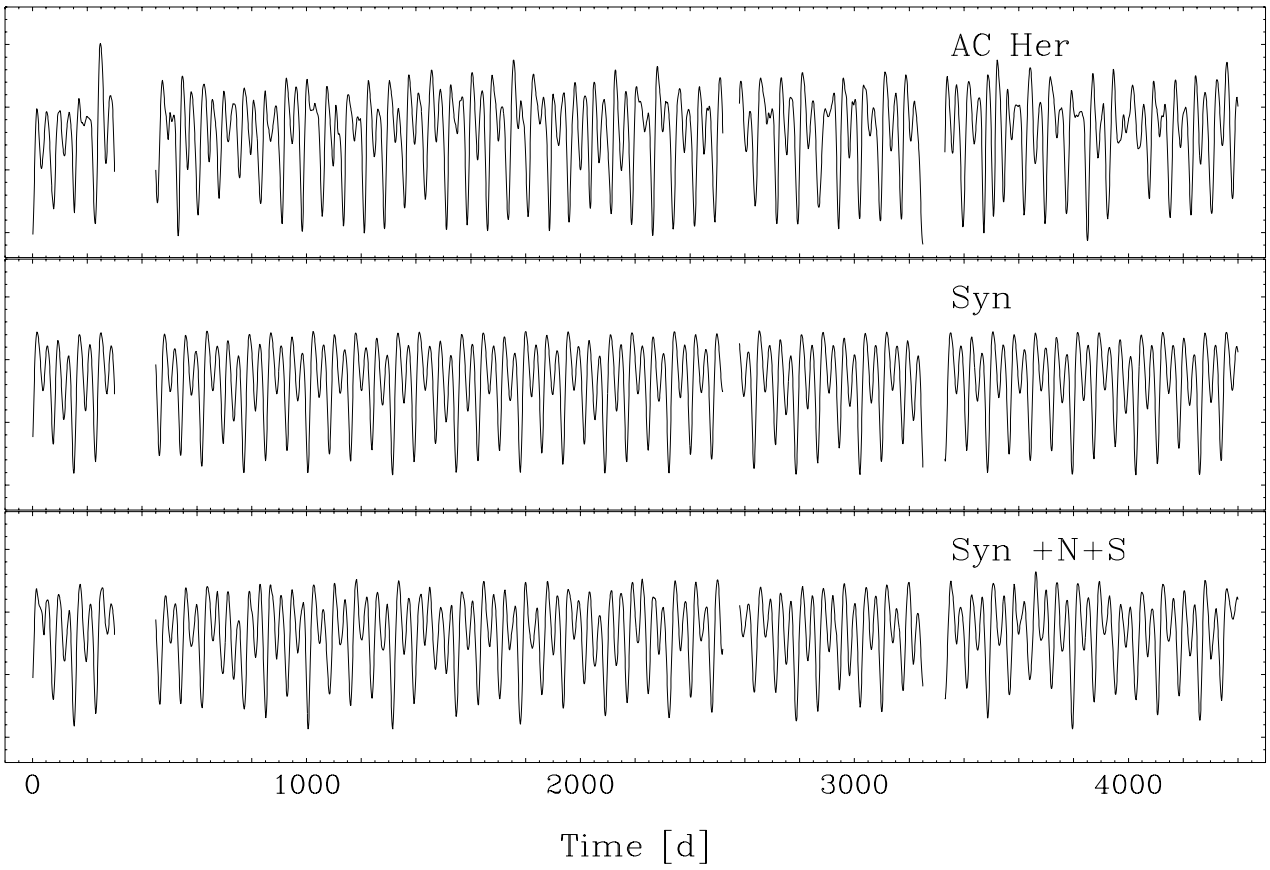
AC Her
Syn
Syn +N+S
0
1000
2000
3000
4000
Time [d]